FUDMA Journal of Sciences (FJS)
ISSN online: 2616-1370
ISSN print: 2645 - 2944
Vol. 10 No. 16, June, 2026, pp 461 – 465
DOI: https://doi.org/10.33003/fjs-2026-1016-5714

A Miniaturized Low-Profile Wearable Dual-Band Patch Antenna for IoT-Enabled Wireless Body Area Networks

***[1]Umar Musa, [2]Abubakar Salisu, [1]Sani Halliru Lawan, [3]Suleiman Aliyu Babale, [1]Suleiman Babani, [2]Kabiru Ibrahim Jahun and [4]Musa Mohammed Bello**

[1]Department of Telecommunications Engineering, Bayero University, Kano State, Nigeria.
[2]Department of Biomedical and Electronics Engineering, University of Bradford, West Yorkshire, United Kingdom.
[3]Department of Electronics and Telecommunications Engineering, Ahmadu Bello University, Zaria, Kaduna State, Nigeria.
[4]Department of Mechatronics Engineering, Bayero University, Kano State, Nigeria.

*Corresponding authors' email: umusa.ele@buk.edu.ng

ABSTRACT
A compact low-profile wearable dual-band antenna has been designed and analyzed for Internet of Things (IoT) enabled Wireless Body Area Networks. The proposed antenna is simulated on a Rogers Duroid RO3003 substrate with overall dimensions of 35 × 37 × 0.5 mm³. At the lower operating band of 2.4 GHz, the antenna achieves a −10 dB bandwidth of 4.5%, while at the upper band of 5.8 GHz, a bandwidth of 3.96% is obtained. The radiation patterns are omnidirectional in the H-plane for both frequencies; in the E-plane, bidirectional behaviour is observed at 2.4 GHz and a more directive pattern at 5.8 GHz. Peak gains of 4.6 dBi (2.4 GHz) and 5.9 dBi (5.8 GHz) are obtained, corresponding to radiation efficiencies of 92% and 94%, respectively. Specific Absorption Rate (SAR) evaluation on a multilayer human tissue model yields values of 0.85 W/kg at 2.4 GHz and 0.32 W/kg at 5.8 GHz, all within the safety limits prescribed by international standards. The combination of compact size, dual-band operation, low SAR, and high efficiency makes the proposed antenna a strong candidate for next-generation IoT-WBAN wearable devices.

Received: 10 Aug. 2026
Accepted: 24 Aug. 2026
Published: 02 Sep. 2026

Keywords: Dual-band, IoT, patch antenna, SAR, WBAN

INTRODUCTION
The proliferation of the Internet of Things (IoT) has fundamentally reshaped wireless communication and data acquisition paradigms (Afrin et al., 2025; Yalli et al., 2024). IoT technologies are now pervasive across numerous sectors, including healthcare (remote patient monitoring, vital-sign tracking), defence, smart cities, smart homes, and precision agriculture (Choudhary, 2024; Kumar et al., 2023; Umer et al., 2023). In the healthcare domain specifically, Wireless Body Area Networks (WBANs) have emerged as a key enabler of continuous, real-time patient monitoring outside clinical settings, offering timely data for medical diagnostics and intervention (Musa et al., 2024, 2025).
WBAN devices must satisfy stringent requirements: low cost, minimal power consumption, robustness to body-induced detuning, and comfortable wearability. Depending on the application, WBANs operate in several frequency bands: 400 MHz for implanted medical devices, the Industrial, Scientific and Medical (ISM) bands at 2.4 GHz and 5.8 GHz, and the 3–10 GHz range for Ultra-Wideband (UWB) systems (Yadav et al., 2020). The antenna is a critical component that must function in proximity to or directly on human tissue, and is particularly challenging to design, as the body's electromagnetic properties can significantly alter antenna performance (Shabana et al., 2025; Yahya et al., 2025). Furthermore, wearable antennas must comply with Specific Absorption Rate (SAR) limits set by regulatory bodies such as the ICNIRP and the FCC (Douhi et al., 2025; Dwivedi et al., 2025; Sandhya & Chandra, 2025).
Numerous dual-band wearable antennas have been reported, but many suffer from either a large footprint, narrow bandwidth, suboptimal gain, or relatively high SAR values. In this work, we address these limitations by proposing a miniaturised, low-profile, dual-band patch antenna that operates at both 2.4 GHz and 5.8 GHz. The antenna is realised on a thin (0.5 mm) Rogers RO3003™ substrate, incorporates an inverted-E slot to generate the lower resonance, and achieves excellent radiation efficiency (>91%) while maintaining SAR values well below the safety thresholds. The following sections detail the design evolution, parametric analysis, simulated performance, and a comparative benchmark against state-of-the-art wearable antennas.

MATERIALS AND METHODS
Antenna Design
The antenna is designed and simulated using CST Microwave Studio (CST MWS). A Rogers Duroid RO3003 material is chosen as the substrate because of its stable dielectric constant of 3.0, low loss tangent of 0.0013, and thin profile of 0.5 mm, properties that are highly desirable for wearable applications where flexibility and low weight are important. The development of the proposed antenna follows a two-step process. Initially, a standard rectangular patch antenna is designed to resonate at 5.8 GHz. The dimensions of the patch at 5.8 GHz were calculated using the following steps, as outlined in the transmission line model involving equations (1) – (5). This single-band design provides a reference for the upper resonance.
Step 1: Calculation of width (W) of the patch:

$$W = \frac{c}{2f_o\sqrt{\frac{\varepsilon_e+1}{2}}} \quad (1)$$

Where: c = 3 × 10⁸ m/s
ε_e is the effective dielectric constant
f_0 is the center frequency
Step 2: Calculation of the effective dielectric constant (ε_e):

$$\varepsilon_e = \frac{\varepsilon_r+1}{2} + \frac{\varepsilon_r-1}{2}\left[1 + 12\frac{h}{W}\right]^{-0.5} \quad (2)$$

Where: h is the thickness of the substrate

ε_r Is the relative dielectric constant of the substrate

Step 3: Calculation of the effective length (L_{eff}):

$$L_{eff} = \frac{c}{2f_o\sqrt{\varepsilon_e}} \quad (3)$$

Step 4: Calculation of the length extension (ΔL):

$$\Delta L = 0.412h \frac{(\varepsilon_e+0.3)\left(\frac{W}{h}+0.264\right)}{(\varepsilon_e-0.264)\left(\frac{W}{h}+0.8\right)} \quad (4)$$

Step 5: Calculation of actual length of patch (L):

$$L = L_{eff} - 2\Delta L \quad (5)$$

Step 6: Calculation of substrates dimensions (L_s and W_s): The substrate is six times larger than the height of the dielectric substrate plus the used length or width, as in equations (6) and (7).

$$L_s = 6h + L \quad (6)$$

$$W_s = 6h + W \quad (7)$$

Design Methodology and Key Techniques

To ensure clarity and reproducibility, the overall design strategy is structured into four sequential stages, as illustrated in the methodology flowchart of Fig. 1.

Stage 1 (Input Specifications)

The design begins with defining the operational requirements: dual-band resonance at the 2.4 GHz and 5.8 GHz ISM bands, a compact footprint (target ≤ 35 × 40 mm²), and a low-profile, flexible substrate (Rogers RO3003, h = 0.5 mm) to ensure comfortable wearability.

Stage 2 (Initial Upper-Band Design)

Using the standard transmission-line model, the initial rectangular patch dimensions are analytically calculated via Eqs. 1–5 to resonate at the upper frequency (5.8 GHz). This establishes the primary radiating structure.

Stage 3 (Slot Loading for Dual-Band Operation)

To generate the lower resonance at 2.4 GHz without increasing the antenna's physical size, an inverted E-shaped slot is etched into the radiating patch. This technique effectively lengthens the surface current path, which as per antenna theory, lowers the resonant frequency. The slot acts as a perturbing element that introduces a secondary, well-separated resonance.

Stage 4 (Parametric Optimization)

Critical dimensions of the inverted-E slot (Wslot, Lslot) and the feed position (Wf, Lf) are iteratively optimized using a parametric sweep in CST MWS. The optimization goals are to achieve $|S_{11}| < -10$ dB at both frequencies, maximize radiation efficiency and gain, and minimize the Specific Absorption Rate (SAR) when simulated on a multilayer human tissue model. This systematic approach ensures a balanced trade-off between impedance matching, bandwidth, and radiation performance.

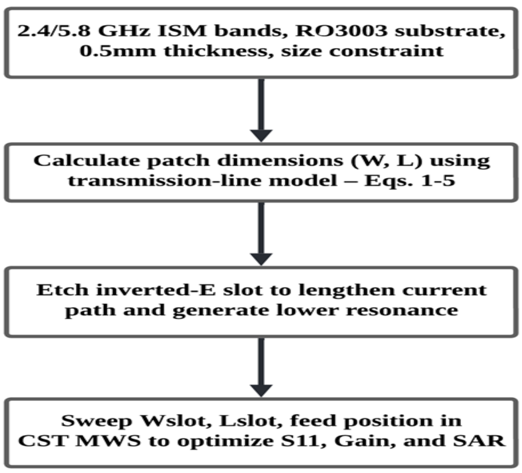

Figure 1: Systematic design methodology flowchart for the proposed dual-band wearable antenna

The final size of the proposed antenna, which was optimized using CST MWS software, is now 35 × 37 × 0.5 mm^3 as seen in Fig. 2. Table 1 lists all dimensions of the final proposed antenna. The values are obtained after an iterative parametric sweep that balances impedance matching, bandwidth, and radiation performance.

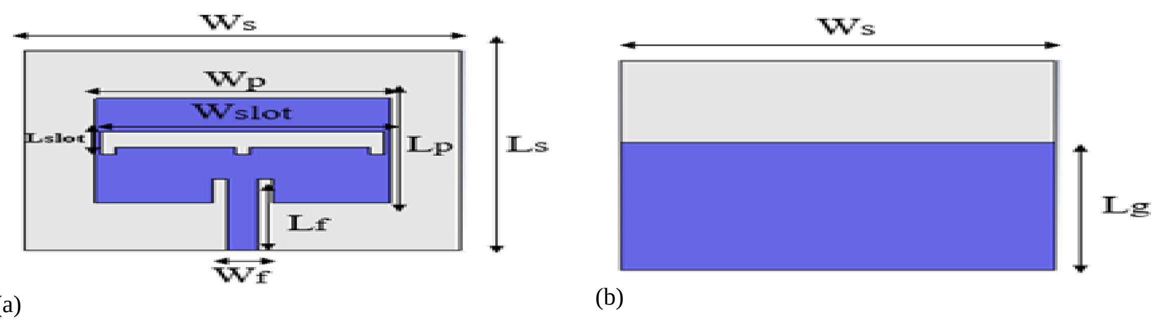

Figure 2: Proposed antenna (a) front (b) back.

Table 1: Proposed Antenna Final Dimensions

Parameters	Value (mm)	Parameters	Value (mm)
Ls	35	Wf	2.7
Ws	37	Lf	11
Wp	26	Wslot	23
Lp	18	Lslot	4

RESULTS AND DISCUSSION

Fig. 3 shows the simulated S_{11} of the proposed antenna. After incorporating the inverted-E slot, two distinct resonances appear: one at 2.4 GHz and the original one at 5.8 GHz. For the proposed antenna. At the 2.4 GHz band, a −10 dB bandwidth from 2.37 GHz to 2.48 GHz is achieved with a fractional bandwidth of 4.5%. While at the 5.8 GHz band, a −10 dB bandwidth from 5.76 GHz to 5.99 GHz is achieved with a fractional bandwidth of 3.96%. Both bandwidths are sufficient for the intended ISM-band WBAN applications, which typically require only a few percent relative bandwidth.

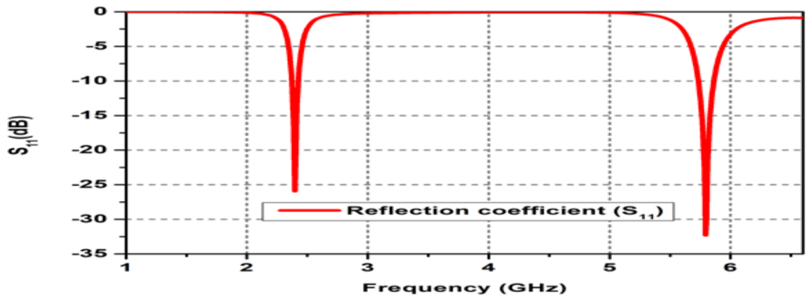

Figure 3: S_{11} of the proposed antenna

Fig. 4 depicts the 2-D radiation patterns at the two resonant frequencies in both principal planes. At 2.4 GHz (Fig. 4a): The H-plane (ϕ = 90°) shows a nearly omnidirectional pattern, which is desirable for on-body communications where the antenna orientation may vary. The E-plane (ϕ = 0°) exhibits a bidirectional pattern, typical of a simple patch antenna operating near its fundamental mode. At 5.8 GHz (Fig. 4b): The H-plane remains omnidirectional, albeit with slightly more ripples due to higher-order mode excitation. The E-plane becomes more bidirectional, with a clear main lobe at θ = 0° (broadside). This bidirectional behaviour at 5.8 GHz can be advantageous for off-body links where a directed beam improves link margin.

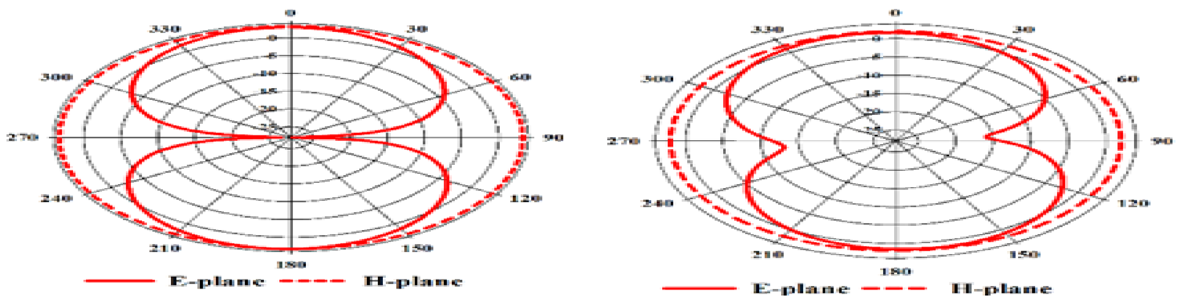

(a) (b)

Figure 4: Radiation Pattern (a) 2.4 GHz (b) 5.8 GHz.

The proposed antenna's simulated gain and efficiency are illustrated in Fig. 5. As seen in Fig. 5(a) and (b), the gain, G (dBi), was determined to be 4.6 dBi and 5.9 dBi at 2.4 GHz and 5.8 GHz, respectively. This results in an efficiency, η (%), of 92% and 94%.

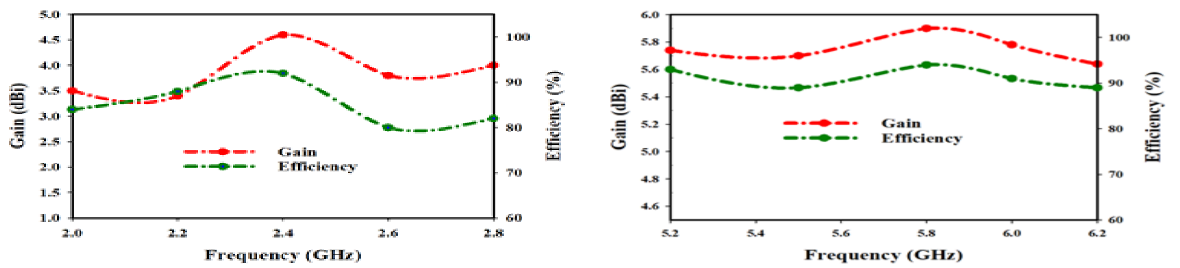

(a) (b)

Figure 5: Gain and efficiency (a) 2.4 GHz (b) 5.8 GHz.

To gain insight into the physical mechanism behind the dual-band operation, the surface current distribution on the patch is examined at each resonance as seen in Fig. 6. at 5.8 GHz as seen in Fig. 6(a), high current density is concentrated along the edges of the main patch and along the microstrip feed line, confirming that the primary patch itself acts as the main radiator for the upper band. The inverted-E slot shows relatively low current intensity at this frequency. At 2.4 GHz, seen in Fig. 6(b), the current is strongly localised around the perimeter of the inverted E-slot, indicating that the slot effectively creates a longer current path. As is known from antenna theory, a longer current path corresponds to a lower resonant frequency (Musa et al., 2023). This observation validates the design strategy: the slot acts as a perturbing element that introduces an additional resonance without increasing the antenna footprint(Ibrahim et al., 2026).

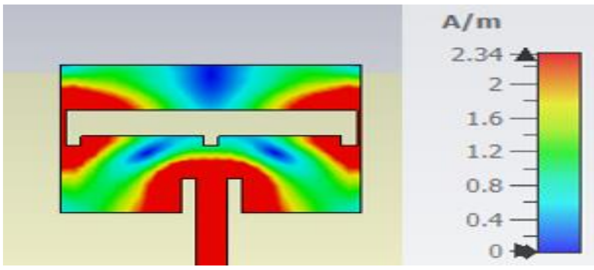

(a)

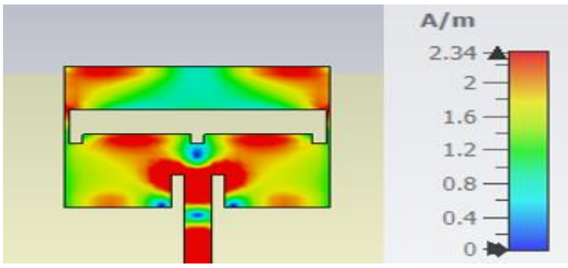

(b)

Figure 6: Current distribution at (a) 2.4 GHz (b) 5.8 GHz

Table 2 benchmarks the proposed antenna against several recently published dual-band wearable antennas. The comparison metrics include physical size, substrate material, operating frequencies, bandwidth, SAR values, and realised gain/efficiency.

Table 2: Performance Comparison with State-Of-The-Art Wearable Dual-Band Antennas

Ref	Size (mm)^2	Material	Freq. (GHz)	BW (%)	SAR (W/kg)	Gain (dBi)/Eff. (%)
(Merugumalli et al., 2025)	40 × 28	Felt	2.4/5.8	29/18	1.37/1.12	2, 4.96/NA
(Bhattacharjee et al., 2019)	50 × 50	Denim	2.4/5.8	1.7/4.2	1.67/1.12	-5.1, 3.3/NA
(Zhao & Geyi, 2020)	50 × 50	FR-4	2.4/5.8	4.2/10.5	1.26/0.46	1.2, 7.9/NA
(Zhou et al., 2020)	100 × 100	Felt	2.4/5.8	4.9/3.8	0.042/0.09	6.33, 6.02/70.1, 72.5
(Ahmad et al., 2021)	40 × 30	FR-4	2.4/3.5	2.04/3.4	0.19/1.18	5.06, 6.33/80, 80
(Mashaghba et al., 2020)	70 × 70	Felt	2.4/3.5	5.3/3.14	NA	NA/29, 48
This work	35 × 37	Rogers	2.4/5.8	4.5/3.96	0.32/0.85	4.6, 5.9/92, 94

CONCLUSION

In this study, a compact, low-profile, dual-band wearable patch antenna for IoT-enabled WBANs, operating at the 2.4 GHz and 5.8 GHz ISM bands using a 0.5 mm Rogers RO3003 substrate with an overall footprint of just 35 × 37 mm². The innovative inverted E-slot enables the lower resonance without enlarging the antenna, yielding fractional bandwidths of 4.5% and 3.96%, omnidirectional H-plane patterns, high radiation efficiencies of 92% and 94%, gains of 4.6 dBi and 5.9 dBi, and SAR values well within safety limits of 0.32 W/kg at 5.8 GHz, and 0.85 W/kg at 2.4 GHz. Compared to recent state-of-the-art designs, this antenna offers an attractive balance of small size, high efficiency, good gain, and low SAR, making it a strong candidate for next-generation WBAN applications such as remote health monitoring, fitness tracking, and emergency response.

REFERENCES

Afrin, S., Rafa, S. J., Kabir, M., Farah, T., Alam, M. S. Bin, Lameesa, A., Ahmed, S. F., & Gandomi, A. H. (2025). Industrial Internet of Things: Implementations, challenges, and potential solutions across various industries. Computers in Industry, 170, 104317. https://doi.org/https://doi.org/10.1016/j.compind.2025.104317

Ahmad, S., Ghaffar, A., Hussain, N., & Kim, N. (2021). Compact Dual-Band Antenna with Paired L-Shape Slots for On- and Off-Body Wireless Communication. Sensors, 21(23). https://doi.org/10.3390/s21237953

Bhattacharjee, S., Maity, S., Chaudhuri, S. R. B., & Mitra, M. (2019). A Compact Dual-Band Dual-Polarized Omnidirectional Antenna for On-Body Applications. IEEE Transactions on Antennas and Propagation, 67(8), 5044–5053. https://doi.org/10.1109/TAP.2019.2891633

Choudhary, A. (2024). Internet of Things: a comprehensive overview, architectures, applications, simulation tools, challenges and future directions. Discover Internet of Things, 4(1), 31. https://doi.org/10.1007/s43926-024-00084-3

Douhi, S., Houssaini, Y., Das, S., Subramanian, V., Madhav, B. T. P., Mazroui, M. 'hamme., & Eddiai, A. (2025). Metamaterial-integrated wearable UWB antenna with SAR reduction and gain enhancement for Wireless Body Area Sensor Networks (WBASNs): Design and experimental verification. Sensors and Actuators A: Physical, 388, 116499. https://doi.org/https://doi.org/10.1016/j.sna.2025.116499

Dwivedi, R., Srivastava, D., & Singh, V. (2025). Wearable Textile Antenna with Low SAR and High Fidelity for BAN and Medical Applications. International Journal of Numerical Modelling: Electronic Networks, Devices and Fields, 38. https://doi.org/10.1002/jnm.70058

Ibrahim, I., Aliyu, S., Halliru Lawan, S., & Aminu Abubakar, A. (2026). FUDMA Journal of Engineering and Technology Design of a Modified Wideband Microstrip Patch Antenna for WLAN/WiMAX Applications. Journal of Engineering and Technology, Volume 2, 2026, 989–999.

Kumar, M., Kumar, A., Verma, P., Bhattacharya, P., Ghimire, D., Kim, S., & Hosen, A. S. M. (2023). Healthcare Internet of Things (H-IoT): Current Trends, Future Prospects, Applications, Challenges, and Security Issues. Electronics, 12. https://doi.org/10.3390/electronics12092050

Mashaghba, H. A., Rahim, H. A., Soh, P. J., Abdulmalek, M., Adam, I., Jusoh, M., Sabapathy, T., Yasin, M. N. M., & Rani, K. N. A. (2020). Bending Assessment of Dual-band Split Ring-shaped and Bar Slotted All-Textile Antenna for Off-body WBAN/WLAN and 5G Applications. 2020 2nd International Conference on Broadband Communications, Wireless Sensors and Powering (BCWSP), 1–5. https://doi.org/10.1109/BCWSP50066.2020.9249403

Merugumalli, R. K., Murugan, N. A., & Chalasani, S. R. (2025). Design and optimization of a compact dual-band antenna using artificial neural networks for body area network applications. AEU - International Journal of Electronics and Communications, 200, 155911. https://doi.org/https://doi.org/10.1016/j.aeue.2025.155911

Musa, U., Shah, S. M., Majid, H. A., Mahadi, I. A., Rahim, M. K. A., Yahya, M. S., & Abidin, Z. Z. (2023). Design and Analysis of a Compact Dual-Band Wearable Antenna for WBAN Applications. IEEE Access, 11, 30996–31009. https://doi.org/10.1109/ACCESS.2023.3262298

Musa, U., Shah, S. M., Majid, H. A., Mahadi, I. A., Rahim, M. K. A., Yahya, M. S., & Abidin, Z. Z. (2024). Design and Implementation of Active Antennas for IoT-Based Healthcare Monitoring System. IEEE Access, 12, 48453–48471. https://doi.org/10.1109/ACCESS.2024.3384371

Musa, U., Smida, A., Yahya, M. S., Waly, M. I., Tiang, J. J., Mallat, N. K., Muhammad, S., & Salisu, A. (2025). Machine learning-optimized dual-band wearable antenna for real-time remote patient monitoring in biomedical IoT systems. Scientific Reports, 15(1), 30943. https://doi.org/10.1038/s41598-025-15984-9

Sandhya, R., & Chandra, A. (2025). A Compact Tree-Shaped Dual-Band Wearable Antenna with Enhanced Far-Field Performance for WBAN Applications. IEEE Access, 13, 152241–152252. https://doi.org/10.1109/ACCESS.2025.3604551

Shabana, A., El-Bakry, A., & Mahdy, S. (2025). Implantable antenna for biomedical applications: electromagnetic, SAR, and thermal performance evaluation. Scientific Reports, 15(1), 35404. https://doi.org/10.1038/s41598-025-21600-7

Umer, M., Aljrees, T., Karamti, H., Ishaq, A., Alsubai, S., Omar, M., Bashir, A. K., & Ashraf, I. (2023). Heart failure patients monitoring using IoT-based remote monitoring system. Scientific Reports, 13(1), 19213. https://doi.org/10.1038/s41598-023-46322-6

Yadav, A., Singh, V., Marques, G., Zapirain, B., & la Torre Díez, I. (2020). Wireless Body Area Networks: UWB Wearable Textile Antenna for Telemedicine and Mobile Health Systems. Micromachines, 11. https://doi.org/10.3390/mi11060558

Yahya, M. S., Musa, U., Zidan, M. S., Soeung, S., Izhar, L. I., Zakaria, Z., & AL-Gburi, A. J. A. (2025). Machine learning-optimized compact dual-band medical syringe-inspired wearable antenna for efficient WBAN applications. Scientific Reports, 15(1), 43240. https://doi.org/10.1038/s41598-025-27227-y

Yalli, J., Hasan, M., & Badawi, A. (2024). Internet Of Things (IOT): Origins, Embedded Technologies, Smart Applications and its Growth in the Last Decade. IEEE Access, 12, 91357–91382. https://doi.org/10.1109/ACCESS.2024.3418995

Zhao, C., & Geyi, W. (2020). Design of a dual band dual mode antenna for on/off body communications. Microwave and Optical Technology Letters, 62(1), 514–520. https://doi.org/https://doi.org/10.1002/mop.32085

Zhou, L., Fang, S., & Jia, X. (2020). Dual-band and dual-polarised circular patch textile antenna for on-/off-body WBAN applications. IET Microwaves, Antennas \& Propagation, 14(7), 643–648. https://doi.org/https://doi.org/10.1049/iet-map.2019.1073